ARTICLE

ABC Triblock Copolymer Vesicles with Mesh-Like Morphology

Wei Zhao, Dian Chen, Yunxia Hu, Gregory M. Grason,* and Thomas P. Russell*

Department of Polymer Science and Engineering, University of Massachusetts, Amherst, Massachusetts 01003, United States

ABSTRACT Polymer vesicles made from poly(isoprene-*b*-styrene-*b*-2-vinyl pyridine) (PI-*b*-PS-*b*-P2VP) triblock copolymer confined within the nanopores of an anodic aluminum oxide (AAO) membrane are studied. It was found that these vesicles have well-defined, nanoscopic size, and complex microphase-separated hydrophobic membranes, comprised of the PS and PI blocks, while the coronas are formed by the P2VP block. Vesicle formation was tracked using both transmission and scanning electron microscopy. A mesh-like morphology formed in the membrane at a well-defined composition of the three blocks that can be tuned by changing the copolymer composition. The nanoscale confinement, copolymer composition, and subtle molecular interactions contribute to the generation of these vesicles with such unusual morphologies.

KEYWORDS: block copolymer · vesicle · anodic aluminum oxide · ethylene glycol · morphologies

In recent decades, the morphologies formed by polymeric amphiphiles have been widely studied. Bilayers, cylinders, and spheres form spontaneously when dispersed in water, depending on the size and shape of the hydrophobic and hydrophilic portion of the macromolecules.[1] Among all those motifs, vesicles play a special role as synthetic mimics of lipid-based living cell membranes. Block copolymer vesicles (polymersomes) exhibit superior mechanical and physical properties compared to lipid-based vesicles. Higher copolymer molecular weights lead to increased bending rigidities and critical areal strain before rupture as well as the membrane permeability.[2−4] Based on these properties, polymeric vesicles hold promise for many potential applications in areas such as drug delivery, microreactors, and microcapsules.[5−9]

ABC triblock copolymer vesicles have been investigated as mimics of natural membranes, most of which are asymmetric to help orient membrane proteins to fulfill their biological function.[10−13] The introduction of three different blocks provides additional means to manipulate the size, shape, and stability of the vesicle structure. Stoenescu *et al*. reported the forming of asymmetric membranes in poly(ethylene oxide)-*b*-poly(dimethyl siloxane)-*b*-poly(methyl oxazoline) (PEO-*b*-PDMS-*b*-PMOXA) triblock copolymer, which has been shown to properly orient a trans-membrane protein.[10,11] Biocompatible asymmetric membranes have also been reported for poly(ethylene oxide)-*b*-poly(caprolactone)-*b*-poly-(acrylic acid) (PEO-*b*-PCL-*b*-PAA) triblock copolymers.[12] Liu *et al*. studied the change of aggregate morphologies of the biamphiphilic triblock poly(acrylic acid)-*b*-polystyrene-*b*-poly(4-vinyl pyridine) (PAA-*b*-PS-*b*-P4VP) as a function of pH in DMF/THF/H_2O mixtures and found a reversible conversion from vesicles (pH around 1) to solid spherical or ellipsoidal aggregates (pH from 3 to 11) and finally back to vesicles (pH around 14).[13] Brannan *et al*. also achieved asymmetry in vesicle membranes by using an ABCA copolymer poly(ethylene oxide)-*b*-polystyrene-*b*-polybutadiene-*b*-poly(ethylene oxide) (PEO-*b*-PS-*b*-PBD-*b*-PEO), which was attributed to the high interfacial tension between PBD and water causing the former chains located toward the inner leaflet.[14]

Polymer vesicles are commonly generated using methods like solvent switching, film rehydration, electroformation, and microfluidics.[15,16] On the other hand, numerous polymer nanostructures can be produced using porous templates, like anodic aluminum oxide (AAO) membranes. These membranes are characterized by their narrow pore size distribution and regular arrangement of the pores.[17] Currently accessible pore diameters range from 8 to 500 nm, which enable the systematic variation of the degree of confinement from nearly

*Address correspondence to grason@mail.pse.umass.edu, russell@mail.pse.umass.edu.

Received for review September 3, 2010 and accepted November 19, 2010.

Published online December 3, 2010. 10.1021/nn1028289

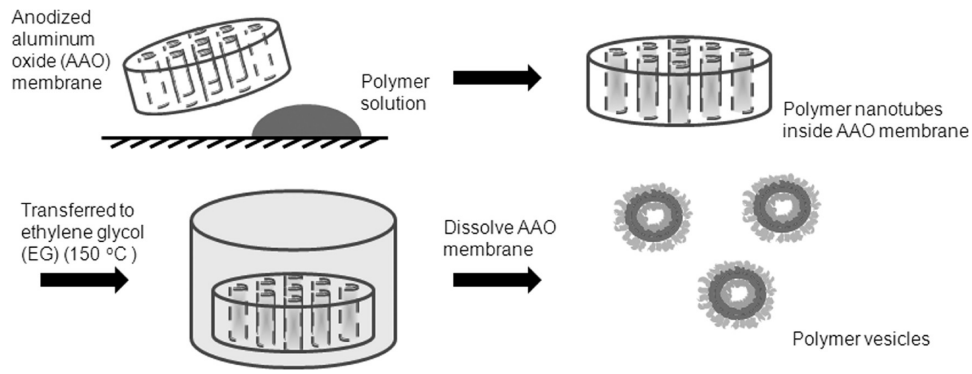

Scheme 1. Sample Preparation Process.

bulk to highly confined, *i.e.*, to dimensions smaller than the radius of gyration. By tuning the confinement and the surface properties of the cylindrical pore, nanorods of polystyrene-*b*-polybutadiene (PS-*b*-PBD), polystyrene-*b*-poly(4-vinyl pyridine) (PS-*b*-P4VP), and polystyrene-*b*-poly(methyl methacrylate) (PS-*b*-PMMA) have been prepared within AAO membranes, and the resultant morphologies were studied.[18−22] Novel morphologies, including helices and stacked toroids, were obtained due to the forced curvature and the confinement induced entropy loss.[19,23,24] In addition, porous nanotubes[25−29] and other mesoporous nanostructures[30−34] were produced using AAO membranes from other copolymers, including polystyrene-*b*-polyacrylonitrile (PS-*b*-PAN), PS-*b*-P4VP, and poly(ethylene oxide)-*b*-poly(propylene oxide)-*b*-poly(ethylene oxide) (PEO-*b*-PPO-*b*-PEO).

However, the potential use of AAO membranes to guide and control the formation of polymer vesicles has not been well studied. Previously Chen *et al.* reported a promising method to make mesoporous nanostructures by annealing block copolymer materials within the confinement of AAO membrane nanopores.[32] Here we further explored the use of this method in making polymer vesicles. A schematic diagram of the sample preparation is shown in Scheme 1. Polyisoprene[1,4-addition]-*b*-polystyrene-*b*-poly(2-vinyl pyridine) (PI-*b*-PS-*b*-P2VP) triblock copolymer vesicles with relatively uniform size were produced within the nanopores of AAO membranes. Moreover, these vesicles were found to have a unique mesh-like morphology inside the hydrophobic membrane (Figure 1A). This morphology, more than likely, arises from the copolymer composition and the moderate volume fraction of PI block in the PI-*b*-PS-*b*-P2VP copolymer. We found the morphologies to be extremely sensitive to changes in molecular weight and composition of triblock copolymer. This process offers a simple way to fabricate block copolymer vesicles with tunable uniform size and complex structures interior to the bilayer of a well-controlled length scale, which could be further utilized as nanostructured templates.

RESULTS AND DISCUSSION

Typical morphologies of PI-*b*-PS-*b*-P2VP (IS2VP80k) triblock copolymer generated after 5 min heating of the AAO membrane in ethylene glycol are shown in Figure 1. The transmission electron microscopy (TEM) image in Figure 1A shows a vesicular structure, exhibiting a red blood cell-like shape, as shown in the scanning electron microscopy (SEM) image of Figure 1B. This concave shape indicates that a hollow structure (vesicle)

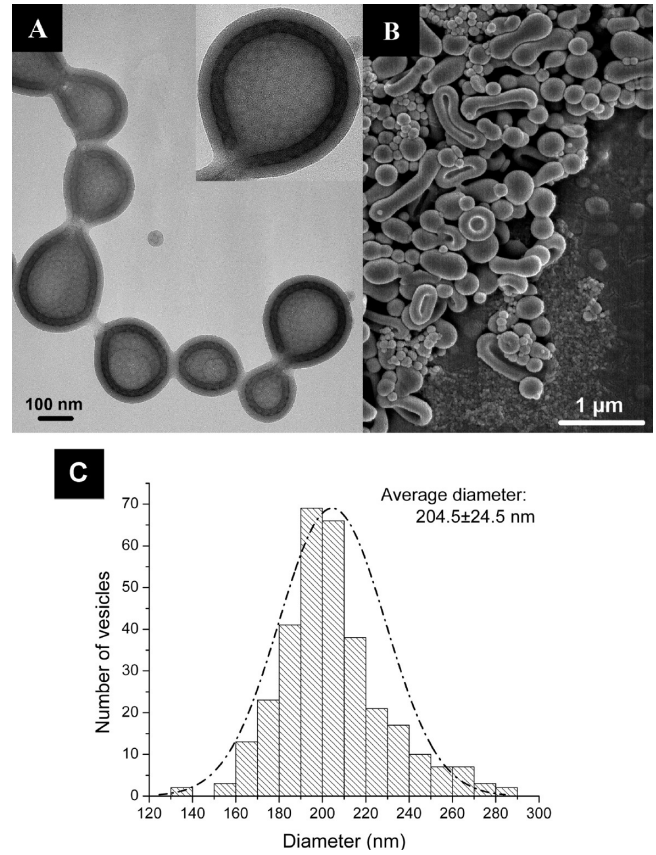

Figure 1. Electron micrographs of a typical vesicle structure generated from IS2VP80k triblock copolymer in 200 nm AAO membrane: (A) TEM image of vesicles with PI microphase selectively stained by OsO_4. Most of the hollow vesicular shape remains stable due to the fact that after quenching the temperature is below T_g of PS block, which forms the major part of the hydrophobic membrane. Insert: zoomed-in view of one vesicle, showing the fine morphology inside the hydrophobic layer. (B) SEM image of the same vesicles and (C) size distribution of vesicles obtained from the SEM images.

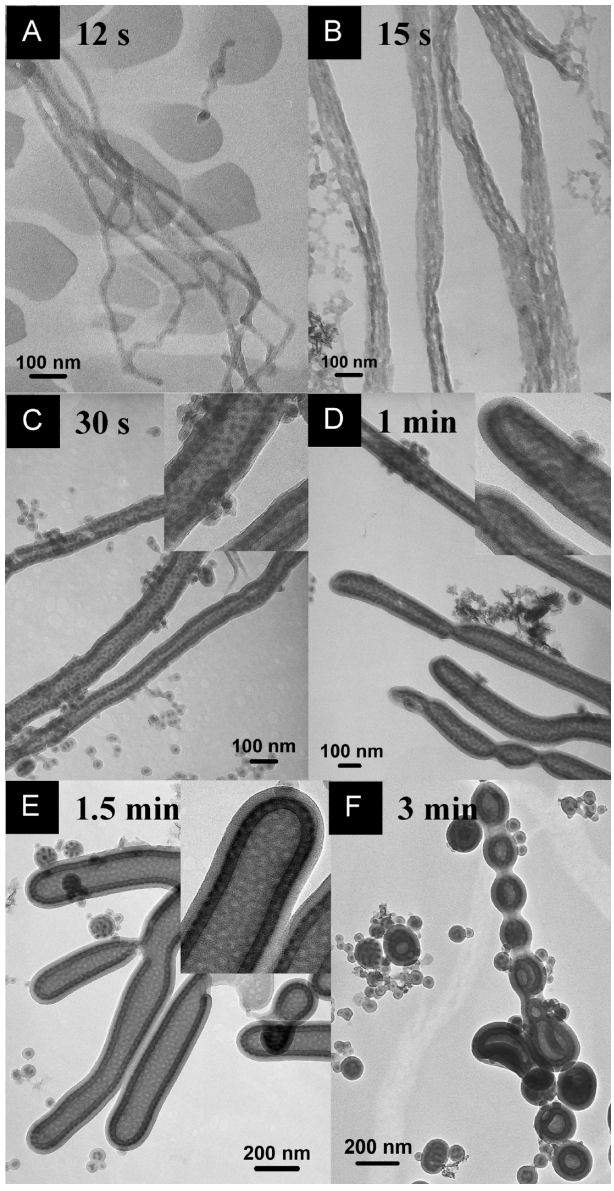

Figure 2. TEM images of structures generated from IS2VP80k triblock copolymer within confinement of 200 nm AAO membrane nanopores after heating in ethylene glycol for different periods of time: (A) 12 s, (B) 15 s, (C) 30 s (inserted with zoomed-in view), (D) 1 min (inserted with zoomed-in view), (E) 1.5 min (inserted with zoomed-in view) and (F) 3 min. All the samples were prepared by dropping suspension solution onto copper grids, dried, and then selectively stained by OsO_4.

formed during the process collapsed upon drying. The histogram in Figure 1C reflects a moderately narrow size distribution with an average diameter of 204.5 nm, which is consistent with the mean diameter of the nanopores in the membrane. Here the data are gathered from several SEM images, and both spherical and cylindrical diameters of the vesicles are counted. Vesicular structures were generated, since ethylene glycol is a selective solvent for the P2VP block at elevated temperatures,[32] and the volume fraction of P2VP block in this triblock copolymer IS2VP80k is only 12.8%. The relatively short P2VP block biases the formation of bilayered (vesicle) structures in a selective solvent, consistent with the results for PS-*b*-P4VP reported previously.[32] An expanded view of one vesicular morphology reveals a finer morphology formed within the hydrophobic layer. Since OsO_4 was used to selectively stain the PI, while PS remained unstained and appeared light gray in color, the mesh-like morphology indicates microphase separation occurs within the vesicular structure.

A control experiment was performed by directly dispersing a bulk sample of IS2VP80k in ethylene glycol heated at 150 °C for 1 day. Instead of forming vesicles, the bulk copolymer barely dissolved in ethylene glycol. We also investigated the structural evolution inside the nanopores of the AAO membrane by changing the heating time at 150 °C from several seconds to 5 min. After quenching in ethylene glycol at temperatures below the glass-transition temperature (T_g) of PS and P2VP (~100 °C), structures at different stages were kinetically trapped and released from AAO membranes for characterization.

The resultant structures formed at different times are shown in Figure 2. As the starting point, the block copolymer solutions were drawn into the nanopores of AAO membrane by capillary action and, after solvent evaporation, left as a thin layer deposited onto the walls of the nanopores. Upon exposure to ethylene glycol at high temperature (150 °C), which is a selective solvent for the P2VP block, for just 12 s, the IS2VP80k dissolved and formed cylindrical micelles inside the nanopores of the membrane. As shown in Figure 2A, these cylindrical micelles are separated and disperse after release from the membrane. However, after a few more seconds of heating, the cylindrical micelles began to fuse together. Because of this, a tubular shape was obtained, as shown in Figure 2B, even after separation from the AAO membrane. After longer heating times, hollow tubes formed, as shown in Figure 2C. The tube diameter is ~100 nm, similar to the size of cylindrical micelle bundles shown in Figure 2B and much smaller than the nanopore diameter (~200 nm). Moreover, the tube ends remained open at this stage, and microphase separation began to take place. In Figure 2C, the PI microphase is shown as isolated black dots and lines dispersed in a gray PS matrix. In the next stage, the tube ends closed, presumably to minimize the free energy cost associated with vesicle edges, as shown in Figure 2D. The tube diameter and microphase separated morphology remained almost the same as in the previous stage, but the distribution of PI microdomains changed from being a random dispersion along the entire hydrophobic membrane thickness in Figure 2C to a concentrated layer shifted away from the outer edge of the membrane. After another 30 s of heating, the tube diameter, as shown in Figure 2E, increased to ~200 nm, which is equal to the size of the nanopores in the AAO membrane. The morphology also changed during the swelling process, where the concentrated, but still

isolated, PI layer changed from being continuous to a layer perforated with holes. This is the morphology ultimately observed in the vesicles. Fluid cylinders are unstable to long-wavelength surface fluctuations and generally undergo a Rayleigh instability in which they break into spherical drops.[29,32] Indeed, we observed that the tubules became wavy or undulated along the tube axis, while the internal morphology remained unchanged, as shown in Figure 2F. With even longer heating time, the undulating tubes broke into spheres or shorter tubes, resulting in the vesicle structures of the final stage.

Expansions of the TEM images in Figure 2D and E lead to the following question: Does the apparent asymmetry along the direction across the hydrophobic membrane come from an asymmetric structure? We know that asymmetry may be due to a real asymmetric structure or a particular direction of projection of three-dimensional structures onto a two-dimensional plane. To further investigate the inner morphology of the hydrophobic membrane, microtomed cross sections were obtained, and the TEM images are shown in Figure 3. The first two images show the morphology obtained in the hydrophobic membrane of IS2VP80k tubes confined within the AAO membrane after heating in ethylene glycol for 1 min. In Figure 3A, PI was selectively stained, and the microdomains appeared as dark dots and lines. Then P2VP block was subsequently stained and appeared as gray regions around the PI domains in Figure 3B. From a comparison of these two images, it is evident that there is a P2VP corona on both sides of the hydrophobic layer, further evidence of the vesicle structure. In addition, the small white gap between the P2VP region and the PI lines in Figure 3B indicates the presence of PS layers on both sides of the continuous PI layer. The presence of the continuous PI layer is further supported by the results in Figure 3C and D, which shows the morphology obtained from IS2VP80k samples after heating in ethylene glycol for 5 min. A dark mesh-like layer with white holes inside is seen in Figure 3C, and a diffuse gray region around the edge after the P2VP was stained (Figure 3D). Since OsO_4 only stains PI, the dark mesh is PI, and the white holes are PS perforating the middle PI layer.

Based on these results, the morphology can be described as: P2VP chains form corona on both sides of the hydrophobic membrane in the vesicle; and PI with the PS form the hydrophobic membrane, with PI comprising a continuous mesh layer sandwiched and perforated by PS. This is shown schematically in Scheme 2. The observation that the PI block remains between two PS layers can be attributed to two factors. First is the higher interfacial tensions of PI and ethylene glycol, in comparison to PS and ethylene glycol,[14] and the second is the sequencing of the three blocks, where PS is the center block bridging between the PI and P2VP blocks. This architecture essentially excludes the formation of an asymmetric hydrophobic membrane in the vesicle with a selective solvent for P2VP present, strongly favoring the formation of a double-layered membrane with the block copolymer, arranged as P2VP−PS−PI−PI−PS−P2VP. The apparent asymmetry shown in Figures 1A and 2D and E results from the projection of a three-dimensional, symmetric bilayer structure onto a two-dimensional image plane. The formation of the perforated PI morphology is due to the specific composition of PI in PI-*b*-PS-*b*-P2VP triblock copolymer, which is only 12.8% (by volume).

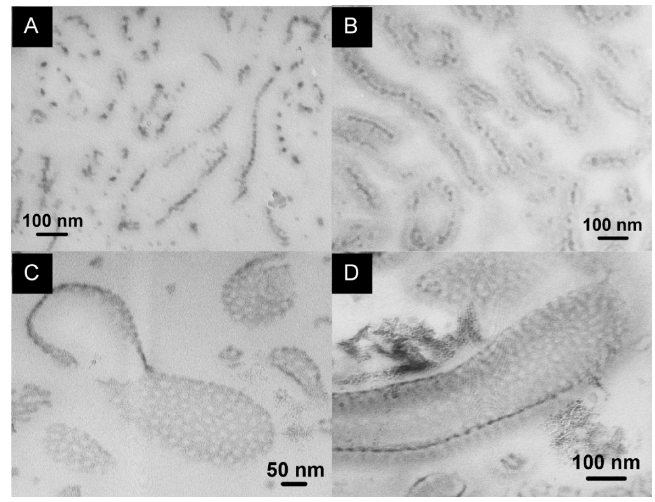

Figure 3. TEM images of morphologies in the hydrophobic membranes of structures generated from IS2VP80k triblock copolymer within confinement of 200 nm AAO membrane nanopores after heating in ethylene glycol for: (A and B) 1 min and (C and D) 5 min. All the samples were prepared by microtoming, while (A and C) were stained by OsO_4 where PI microdomains appear to be dark, and (B and D) were further stained from (A), and (C) separately by $C_4H_8I_2$, where P2VP microdomains appear to be gray and PI remains dark.

To support this model for the meshed structure formed inside the hydrophobic membrane, two additional sets of experiments were performed. First, we used PI-*b*-PS-*b*-P2VP triblock copolymers with two different molecular weights, IS2VP99k and IS2VP102k,

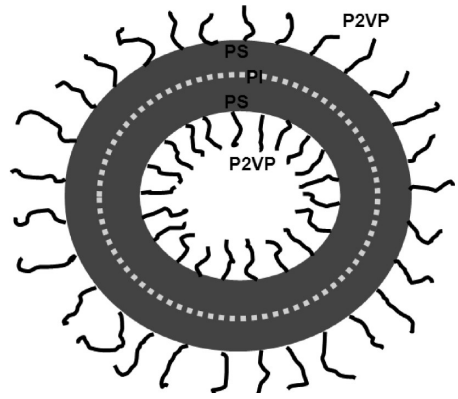

Scheme 2. Schematic of vesicle structure formed from IS2VP80k block copolymer after 5 minute heating in ethylene glycol with confinement of 200 nm AAO membrane. White and gray layers represent PI and PS regions, respectively. Black lines that reside at outer and inner side represent P2VP coronas.

each with a composition similar to the IS2VP80k described above. The volume fractions of PI were 14.9% and 13.9%, respectively. Under identical preparation conditions to generate the vesicular structures from IS2VP80k, these two block copolymers also form vesicles. After selective staining with OsO_4, the morphologies obtained are shown in Figure 4A and B, respectively. In both cases asymmetric hydrophobic membranes were formed with PI in the middle of the membrane. However, in Figure 4B the dark PI layer has only a few perforations, and in Figure 4A no perforations were observed. This can be explained by the increased volume fraction of PI, while maintaining the relative PS and P2VP compositions unchanged. The changes in the number of perforations are directly correlated with variations in the volume fraction of the PI in each of the block copolymers (Table 1). In a second experiment, an AAO membrane with a smaller average nanopore diameter (~100 nm) was used to generate the vesicles shown in Figure 4C. This AAO membrane had a relatively broad pore size distribution and, consequently, the size of vesicles also varied, as seen in Figure 4C. Nevertheless, the morphology produced was the same as that obtained with the 200 nm AAO membrane. This is consistent with the proposed molecular description of these vesicles. Although the number of molecules in one spherical vesicle will increase with increasing diameter, the area that the PI chains need to cover the interface, while forming the middle layer, increases accordingly, assuming a fixed layer thickness. In fact, with an almost fixed hydrophobic membrane and PI middle layer thickness, both the number of molecules and the area of the middle layer scale roughly as the square of the diameter, and thus the area that needs to be covered per chain remains essentially constant. As a result, under the condition that the copolymer composition remains similar, the vesicular structure is maintained, and the PI volume fraction is the only factor that determines the coverage and the morphology in the middle layer. Therefore, we can conclude that the mesh-like middle layer morphology is generated because of the specific amount of PI block in the triblock copolymer IS2VP80k, which can be adjusted by changing the molecular composition, alone.

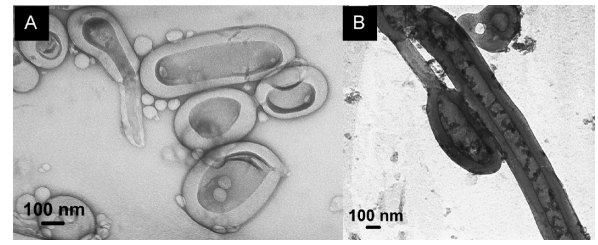

Figure 5. TEM images of: (A) bilayer hollow silica spheres generated by using vesicles obtained from IS2VP80k in 200 nm AAO membrane as scaffold; and (B) vesicles of IS2VP80k block copolymer with ferritin nanoparticles encapsulated. Sample is stained by 2% uranyl acetate$_{(aq)}$ for 30 min.

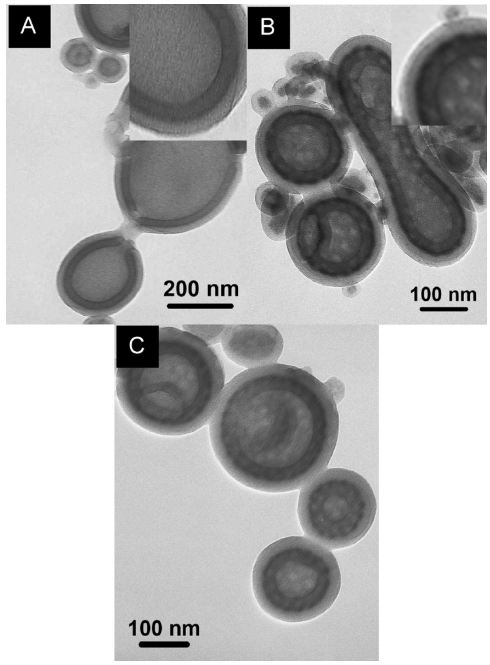

Figure 4. TEM images of vesicles generated from various conditions: (A) IS2VP99k (inserted with zoomed-in view) and (B) IS2VP102k (inserted with zoomed-in view) triblock copolymers within confinement of 200 nm AAO membrane nanopores, and (C) IS2VP80k triblock copolymer within confinement of 100 nm AAO membrane after heating in ethylene glycol for 5 min. All the samples were prepared by dropping suspension solution onto copper grids, drying, and then selectively staining by OsO_4.

Finally, to demonstrate the potential application of these vesicular structures, two experiments were performed. First, they were used as a template for the generation of the corresponding silica nanostructure, as shown in Figure 5A. Copper grids, covered with vesicular structures shown in Figure 1A, were immersed in a hydrolyzed silica precursor solution for 10 min to let the precursor complex with the P2VP chains. The grids were then washed in ethanol for several seconds to remove the excess sol precursor. Subsequently, the copper grids were heated to 400 °C in air for 1 h to remove the block copolymer surfactant, and the block copolymer template bilayered, hollow silica spheres formed, indicating a successful replication. In a second application the vesicular structures were used as solvent-free stable capsules for nanocargo delivery. Ferritin nanoparticles having polyPEGMA ligands were used as a demonstration. An AAO membrane containing IS2VP80k block copolymer nanotubes was immersed and heated at 150 °C in ethylene glycol containing a dispersion of ferritin nanoparticles. As shown in Figure 5B, ferritin was encapsulated within the vesicles and could be retained within the vesicles for a lengthy period of time, and the vesicles could be broken, to deliver the ferritin to a specific targeted area.

TABLE 1. Summary of Triblock Copolymer Compositions and Observed Morphologies

code	M_n, PI (kg/mol)	M_n, PS (kg/mol)	M_n, P2VP (kg/mol)	f_{PI}^{N}	f_{PS}^{N}	f_{P2VP}^{N}	used AAO membrane sizes (nm)	perforation extent
IS2VP80k	9	60	11	0.128	0.746	0.126	100, 200	high
IS2VP102k	12.5	74	15	0.139	0.725	0.136	200	medium
IS2VP99k	13	70	16	0.149	0.703	0.148	200	low

CONCLUSION

The fabrication of PI-*b*-PS-*b*-P2VP triblock copolymer vesicles with novel mesh-like hydrophobic membrane morphology was investigated. Nanoporous AAO membranes were used as templates to guide the fabrication and control the vesicle size. Ethylene glycol, a selective solvent for P2VP block at elevated temperature (150 °C), was used to induce a series of structural and morphological transitions within the confined volume of AAO membranes, from cylindrical micelles to nanotubes to vesicles. The P2VP block forms the coronas of the vesicles surrounding a hydrophobic domain of the PI and PS blocks, with PI forming a meshed middle layer sandwiched between and perforated by two PS layers, where the number of perforations in the mesh could be controlled by controlling the molecular weight and the fraction of the PI block. These hollow vesicular structures are stable at room temperature without solvent for months and can be used as scaffolds for generating inorganic nanostructures or capsules for transporting nanoobjects. These results offer a novel way to generate polymer vesicles of relatively uniform size having adjustable, internal morphologies. The use of this method and the novel morphology as templates to fabricate interesting nanostructures is still under exploration.

EXPERIMENTAL SECTION

Materials. Triblock copolymer PI-*b*-PS-*b*-P2VP with three different molecular weights was used as received from Polymer Source Inc.: PI(9k)-*b*-PS(60k)-*b*-P2VP(11k) (M_n^{PI} = 9, M_n^{PS} = 60, and M_n^{P2VP} = 11 kg/mol), with polydispersity (PDI) of 1.14 (IS2VP80k); PI(12.5k)-*b*-PS(74k)-*b*-P2VP(15k) (M_n^{PI} = 12.5, M_n^{PS} = 74, and M_n^{P2VP} = 15 kg/mol) with polydispersity of 1.17 (IS2VP102k); and PI(13k)-*b*-PS(70k)-*b*-P2VP(16k) (M_n^{PI} = 13, M_n^{PS} = 70, and M_n^{P2VP} = 16 kg/mol) with polydispersity of 1.14 (IS2VP99k). Tetraethyl orthosilicate (TEOS, 98%) was purchased from Acros Organics. The AAO membranes with two different pore diameters were used. A larger membrane has a thickness of ~60 μm and an average pore diameter of ~200 nm, while a smaller one has the same thickness and an average pore diameter of ~100 nm. Both AAO membranes were purchased from Whatman.

Preparation of Vesicles. The ABC triblock copolymers were placed in the AAO membrane from solution. As described previously,[28,29] one drop of the PI-*b*-PS-*b*-P2VP solution (0.5 wt.% in toluene) was placed on glass slide, followed by placing the AAO membrane on top of the solution. Capillary force draws the solution into the membrane instantaneously. After solvent evaporation at ambient conditions, thin films are left on the walls of the nanopores in the AAO membrane. The AAO membrane with the polymer nanotubes inside was immersed in ethylene glycol and heated at 150 °C for several minutes. Vesicles (and other structures) were thus generated inside the nanopores of AAO membrane. After quenching to room temperature, the membrane was dissolved in 5 wt % $NaOH_{(aq)}$, releasing the vesicles that were then collected by filtration. The vesicles were dried in a vacuum oven at 45 °C for 1 day for further characterization.

Preparation of Ceramic Materials. As described previously,[32] a well-established synthetic process was used to generate the silica nanostructure.[35] At first, 2.08 g (0.01 mol) of TEOS was mixed with 3 g of hydrochloric acid (HCl) (0.2 M), 1.8 g of H_2O, and 5 mL of ethanol, and the stirred mixture was heated to 60 °C for 1.5 h to complete the acid-catalyzed hydrolysis−condensation of the silica precursor.[35] Copper grids covered with the PI-*b*-PS-*b*-P2VP vesicular nanostructures were immersed in the hydrolyzed precursor solution for 10 min and washed in ethanol for a few seconds to remove excess sol precursor. Subsequently, the copper grids were heated to 400 °C in air for 1 h to remove the block copolymer surfactant. In so doing, the PI-*b*-PS-*b*-P2VP vesicular nanostructures were successfully replaced by silica.

Preparation of PolyPEGMA-Grafted Ferritin Nanoparticles.[36] Atom-transfer radical polymerization (ATRP) was used to grow poly(ethylene glycol) methacrylate (PEGMA) from the surface of ferritin to improve the stability of the bionanoparticles. Ferritin macroinitiator was prepared first by amidation of NHS-functionalized tertra(ethylene glycol) isobutyl bromide initiator with surface-available amines. Polymerization from ferritin macroinitiator was performed in aqueous solution with CuBr and 2,2′-bipyridine (bpy), using PEGMA (M_n: 475 g/mol) monomers with the feed ratio of monomer over initiator 50. CuBr and bpy were added to a degassed ferritin macroinitiator solution, followed by an addition of a degassed aqueous solution of PEGMA. Passage of the reaction mixture over a Sephadex G-25 column gave the polyPEGMA-grafted ferritin nanoparticles as pure conjugates. The final polymer grafted ferritin nanoparticles are 17 nm in diameter with 45 of polymer chains (5.7 kDa per chain).

Characterization. A SEM (JEOL 6320) with an accelerating voltage of 5 kV was used to investigate the nanostructures. Samples were coated with 2 nm of Au before performing SEM measurements. Bright-field TEM studies were conducted with a JEOL 2000 FX TEM operated at an accelerating voltage of 200 kV. For TEM, part of the samples were placed onto Formvar-coated copper grids and selectively stained by osmium tetroxide (OsO_4), 1,4-diiodobutane, or uranyl acetate. Other samples were embedded in an epoxy resin which was purchased from Polysciences and consisted of three components: araldite resin, dodecenylsuccnic anhydride, and DMP-30. After curing the resin at 60 °C for 24 h, the samples were cut into thin sections by using a Leica Ultracut microtome equipped with a diamond knife. TEM studies were then performed after selective staining.

Acknowledgment. This work was supported by the U.S. Department of Energy (DOE), and the NSF supported MRSEC at the University of Massachusetts Amherst.

Supporting Information Available: This material is available free of charge via the Internet at http://pubs.acs.org.

REFERENCES AND NOTES

1. Israelachvili, J. *Intermolecular & Surface Forces*, 2nd ed.; Academic Press: London, 1991.
2. Discher, B. M.; Won, Y. Y.; Ege, D. S.; Lee, J. C.; Bates, F. S.;

Discher, D. E.; Hammer, D. A. Polymersomes: Tough Vesicles Made from Diblock Copolymers. *Science* **1999**, *284*, 1143–1146.
3. Bermudez, H.; Brannan, A. K.; Hammer, D. A.; Bates, F. S.; Discher, D. E. Molecular Weight Dependence of Polymersome Membrane Structure, Elasticity, and Stability. *Macromolecules* **2002**, *35*, 8203–8208.
4. Rumplecker, A.; Förster, S.; Zähres, M.; Mayer, C. Molecular Exchange through Vesicle Membranes: A Pulsed Field Gradient Nuclear Magnetic Resonance Study. *J. Chem. Phys.* **2004**, *120*, 8740–8747.
5. Ahmed, F.; Pakunlu, R. I.; Srinivas, G.; Brannan, A.; Bates, F. S.; Klein, M. L.; Minko, T.; Discher, D. E. Shrinkage of a Rapidly Growing Tumor by Drug-Loaded Polymersomes: pH-Triggered Release through Copolymer Degradation. *Mol. Pharmaceutics* **2006**, *3*, 340–350.
6. Pang, Z.; Lu, W.; Gao, H.; Hu, K.; Chen, J.; Zhang, C.; Gao, X.; Jiang, X.; Zhu, C. Preparation and Brain Delivery Property of Biodegradable Polymersomes Conjugated with OX26. *J. Controlled Release* **2008**, *128*, 120–127.
7. Lomas, H.; Canton, I.; MacNeil, S.; Du, J.; Armes, S. P.; Ryan, A. J.; Lewis, A. L.; Battaglia, G. Biomimetic pH Sensitive Polymersomes for Efficient DNA Encapsulation and Delivery. *Adv. Mater.* **2007**, *19*, 4238–4243.
8. Broz, P.; Driamov, S.; Ziegler, J.; Ben-Haim, N.; Marsch, S.; Meier, W.; Hunziker, P. Toward Intelligent Nanosize Bioreactors: a pH-Switchable, Channel-Equipped, Functional Polymer Nanocontainer. *Nano Lett.* **2006**, *6*, 2349–2353.
9. Axthelm, F.; Casse, O.; Koppenol, W. H.; Nauser, T.; Meier, W.; Palivan, C. G. Antioxidant Nanoreactor Based on Superoxide Dismutase Encapsulated in Superoxide-Permeable Vesicles. *J. Phys. Chem. B* **2008**, *112*, 8211–8217.
10. Stoenescu, R.; Meier, W. Vesicles with Asymmetric Membranes from Amphiphilic ABC Triblock Copolymers. *Chem. Commun.* **2002**, 3016–3017.
11. Stoenescu, R.; Graff, A.; Meier, W. Asymmetric ABC-triblock Copolymer Membranes Induce a Directed Insertion of Membrane Proteins. *Macromol. Biosci.* **2004**, *4*, 930–935.
12. Wittemann, A.; Azzam, T.; Eisenberg, A. Biocompatible Polymer Vesicles from Biamphiphilic Triblock Copolymers and Their Interaction with Bovine Serum Albumin. *Langmuir* **2007**, *23*, 2224–2230.
13. Liu, F.; Eisenberg, A. Preparation and pH Triggered Inversion of Vesicles from Poly(acrylic acid)-block-polystyrene-block-poly(4-vinyl pyridine). *J. Am. Chem. Soc.* **2003**, *125*, 15059–15064.
14. Brannan, A. K.; Bates, F. S. ABCA Tetrablock Copolymer Vesicles. *Macromolecules* **2004**, *37*, 8816–8819.
15. Battaglia, G.; Ryan, A. J. Pathways of Polymeric Vesicle Formation. *J. Phys. Chem. B* **2006**, *110*, 10272–10279.
16. Hayward, R. C.; Utada, A. S.; Dan, N.; Weitz, D. A. Dewetting Instability during the Formation of Polymersomes from Block-Copolymer-Stabilized Double Emulsions. *Langmuir* **2006**, *22*, 4457–4461.
17. Masuda, H.; Fukuda, K. Ordered Metal Nanohole Arrays Made by a Two-Step Replication of Honeycomb Structures of Anodic Alumina. *Science* **1995**, *268*, 1466–1468.
18. Xiang, H. Q.; Shin, K.; Kim, T.; Moon, S. I.; McCarthy, T. J.; Russell, T. P. Block Copolymers under Cylindrical Confinement. *Macromolecules* **2004**, *37*, 5660–5664.
19. Shin, K.; Xiang, H. Q.; Moon, S. I.; Kim, T.; McCarthy, T. J.; Russell, T. P. Curving and Frustrating Flatlands. *Science* **2004**, *306*, 76.
20. Sun, Y. M.; Steinhart, M.; Zschech, D.; Adhikari, R.; Michler, G. H.; Gösele, U. Confined within Ordered Porous Alumina Templates. *Macromol. Rapid Commun.* **2005**, *26*, 369–375.
21. Dobriyal, P.; Xiang, H. Q.; Kazuyuki, M.; Chen, J. T.; Jinnai, H.; Russell, T. P. Cylindrically Confined Diblock Copolymers. *Macromolecules* **2009**, *42*, 9082–9088.
22. Jeon, S. M.; Lee, Y.; Kim, J. H.; Lee, J. K.; Char, K.; Sohn, B. H. Internal Morphologies of Diblock Copolymer Nanorods Fabricated from Regular and Irregular Pores of Anodized Aluminum Oxide Templates. *React. Funct. Polym.* **2009**, *69*, 558–563.
23. Xiang, H.; Shin, K.; Kim, T.; Moon, S. I.; McCarthy, T. J.; Russell, T. P. The Influence of Confinement and Curvature on the Morphology of Block Copolymers. *J. Polym. Sci., Part B: Polym. Phys.* **2005**, *43*, 3377–3383.
24. Xiang, H.; Shin, K.; Kim, T.; Moon, S. I.; McCarthy, T. J.; Russell, T. P. From Cylinders to Helices upon Confinement. *Macromolecules* **2005**, *38*, 1055–1056.
25. Chen, J. T.; Shin, K.; Leiston-Belanger, J. M.; Zhang, M. F.; Russell, T. P. Amorphous Carbon Nanotubes with Tunable Properties via Template Wetting. *Adv. Funct. Mater.* **2006**, *16*, 1476–1480.
26. Rodriguez, A. T.; Chen, M.; Chen, Z.; Brinker, C. J.; Fan, H. Y. Nanoporous Carbon Nanotubes Synthesized through Confined Hydrogen-Bonding Self-Assembly. *J. Am. Chem. Soc.* **2006**, *128*, 9276–9277.
27. Chen, J. T.; Zhang, M. F.; Yang, L.; Collins, M.; Parks, J.; Avallone, A.; Russell, T. P. Templated Nanostructured PS-*b*-PEO Nanotubes. *J. Polym. Sci., Part B: Polym. Phys.* **2007**, *45*, 2912–2917.
28. Chen, J. T.; Zhang, M. F.; Russell, T. P. Instabilities in Nanoporous Media. *Nano Lett.* **2007**, *7*, 183–187.
29. Chen, D.; Chen, J. T.; Glogowski, E.; Emrick, T.; Russell, T. P. Thin Film Instabilities in Blends under Cylindrical Confinement. *Macromol. Rapid Commun.* **2009**, *30*, 377–383.
30. Wu, Y.; Cheng, G.; Katsov, K.; Sides, S. W.; Wang, J.; Tang, J.; Fredrickson, G. H.; Moskovits, M.; Stucky, G. D. Composite Mesostructures by Nano-Confinement. *Nat. Mater.* **2004**, *3*, 816–822.
31. Wang, Y.; Gösele, U.; Steinhart, M. Mesoporous Block Copolymer Nanorods by Swelling-Induced Morphology Reconstruction. *Nano Lett.* **2008**, *8*, 3548–3553.
32. Chen, D.; Park, S.; Chen, J. T.; Redston, E.; Russell, T. P. A Simple Route for the Preparation of Mesoporous Nanostructures Using Block Copolymers. *ACS Nano* **2009**, *3*, 2827–2833.
33. Wang, K.; Zhang, W.; Phelan, R.; Morris, M. A.; Holmes, J. D. Direct Fabrication of Well-Aligned Free-Standing Mesoporous Carbon Nanofiber Arrays on Silicon Substrates. *J. Am. Chem. Soc.* **2007**, *129*, 13388–13389.
34. Lai, P.; Hu, M. Z.; Shi, D.; Blom, D. STEM Characterization on Silica Nanowires with New Mesopore Structures by Space-Confined Self-Assembly within Nano-Scale Channels. *Chem. Commun.* **2008**, *11*, 1338–1340.
35. Platschek, B.; Petkov, N.; Bein, T. Tuning the Structure and Orientation of Hexagonally Ordered Mesoporous Channels in Anodic Alumina Membrane Hosts: A 2D Small-Angle X-ray Scattering Study. *Angew. Chem., Int. Ed.* **2006**, *45*, 1134–1138.
36. Hu, Y.; Samanta, D.; Parelkar, S. S.; Hong, S. W.; Wang, Q.; Russell, T. P.; Emrick, T. Ferritin-Polymer Conjugates: Grafting Chemistry and Integration into Nanoscale Assemblies. *Adv. Funct. Mater.* **2010**, *20*, 3603–3612.